

Use of an Air Curtain to Reduce Heat Loss from an Inclined Open-Ended Cavity

A. McIntosh¹, G. Hughes² and J. Pye¹

¹College of Engineering and Computer Science,
Australian National University, Canberra ACT 0200, Australia

²Research School of Earth Sciences,
Australian National University, Canberra ACT 0200, Australia

Abstract

The use of an air curtain directed across the aperture of an inclined open-ended cavity is examined as a method to reduce convective losses from a heated cavity. Computational fluid dynamics (CFD) simulations were conducted in two-dimensions for a range of air curtain velocities and axial cavity orientations. The greatest relative reduction in convective losses with an air curtain resulted when the cavity aperture plane was vertical (i.e. horizontal cavity axis). For cavities whose axis was inclined to the horizontal, convective losses could still be lowered with an air curtain, but reduced jet velocities were required for optimum performance.

Introduction

Current applications of air curtains are generally limited to reducing heat transfer between horizontally connected volumes. One example is the commercially available air curtain units commonly fitted to shopfronts. Such units act to suppress the convective exchange of air between a temperature controlled interior environment and an uncontrolled exterior environment. Previous studies, such as the numerical simulations of Costa et al [3], have examined the performance of air curtains in such applications. With a two-dimensional model, Costa recorded a reduction in convective heat transfer of 75-80% under optimum air curtain operation.

The motivation for the current study of air curtains in inclined cavities lies in its application to Concentrating Solar Power (CSP) systems, such as the ANU's Big Dish [2]. An open-ended cavity "receiver" is situated at the focus of a sun-tracking parabolic dish and is used to capture the incident thermal energy. Convective, radiative and conductive heat loss mechanisms all lower the thermal performance of the high-temperature cavity receiver. This study concentrates on the potential to reduce the convective losses.

Taumoefolau [11] and Taumoefolau et al. [12] completed an experimental investigation into the heat loss mechanisms for cavity receivers and found that conductive and radiative losses remain constant with cavity inclination, while convective heat loss is dependent on cavity inclination. Furthermore, Taumoefolau [11] undertook a preliminary investigation of the effects of cross winds on the convective heat loss and found that for low wind speeds (on the order of 0-3 m/s), the convective heat loss was reduced in a manner that was dependent on cavity inclination. These results suggest that the implementation of an air curtain across the aperture of such a cavity may have potential to reduce convective heat loss. The present work utilises a two-dimensional, CFD model to investigate the convective heat transfer mechanisms when introducing an air curtain to an open-ended cavity. A range of cavity inclinations and air curtain velocities are studied.

Model Configuration

The cavity model has a heated interior of width 70mm and depth 150mm, within an insulating enclosure of 290mm diameter and 320mm depth, as shown conceptually in Figure 1. The air curtain was modelled with a 5mm width jet, adjacent to the top vertex of the cavity. The cavity and insulating enclosure was situated within a much larger, closed, ambient domain, as described below. The geometrical configuration is similar to that developed by Paitoonsurikarn [10] to simulate convection in the experiments of Taumoefolau [12]. Unlike Paitoonsurikarn's model, however, the current work uses a two-dimensional simulation (corresponding to a slice in the central plane of the cavity axis) and no turbulent closure scheme, and is implemented with the open-source OpenFOAM CFD Package. In emulating this geometry it was possible to first use the experimental data to provide some validation for the simulations without an air curtain before undertaking simulations that include an air curtain.

The air curtain velocity (V) was defined parallel to the aperture plane of the cavity (perpendicular to the source face of the air curtain), as shown in Figure 1. Acceleration due to gravity (g) was in the negative Y direction, and the axial orientation of the cavity (Θ) was modelled by altering the vector components of gravity relative to the cavity. Cavity inclinations of 0°, 15°, 30°, 45°, 60° and 75° were modelled.

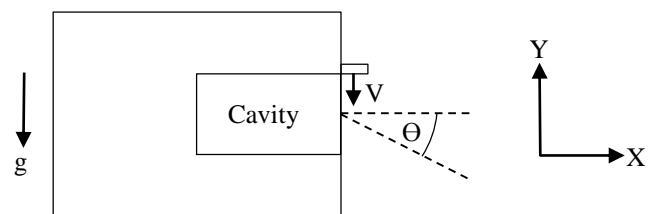


Figure 1. Cavity configuration and variables

Boundary Conditions

Table 1 summarises the boundary conditions used in the studies. The external walls of the cavity enclosure and the face of the air curtain source were adiabatic so that no heat was removed or supplied to the flow there. The much larger ambient domain was closed and taken to be 7m × 7m with no-slip walls held at 300K. This domain size was commensurate with that suggested by Paitoonsurikarn et al. [10] for invariance of the simulated flow in the cavity.

The air curtain was specified to be an inlet jet with a locally perpendicular velocity component and a temperature equal to the ambient (300K); a heated air curtain was not studied. The heated cavity interior was set at a uniform temperature of 720K, which allowed for comparison of results with Paitoonsurikarn's work.

Region	Temperature	Velocity
Inner Cavity Wall	720K	0 m/s
Air Curtain Face	300K	[0, V, 0]m/s
External Cavity and Air Curtain Source faces	Adiabatic	0 m/s
Domain Walls	300K	0 m/s

Table 1. Boundary Conditions

Fluid Properties

The fluid properties were set (and remained constant) for an assumed film temperature of 510K. Estimates of these properties were obtained through linear interpolation of data from Holman [7]. The specific heat capacity (C_p) was set at 1.0314 kJ/kg K, dynamic viscosity (μ) was set at 2.7064×10^{-5} kg/m s and the Prandtl number (Pr) at 0.68.

OpenFOAM Solver

OpenFOAM Version 2.1.1 was used in this investigation. The native “buoyantPimpleFoam” solver was selected; it combines the Simple Algorithm and PISO Algorithm to enable simulation of transient, compressible flows with buoyancy forces [8]. Note that a compressible solver was necessary due to the single inlet represented by the air curtain. Given the maximum simulated air curtain velocity was 2 m/s, the mass added to the closed domain by the air curtain was less than 0.5% of the total. This mass addition was assumed to have a negligible effect on the pressure field within the simulation and to be of lesser dynamic consequence than other approximations used in this study.

Throughout these simulations the Courant number was set to 0.9 and this provided solutions that were independent of time step to within 5%. The convergence residuals for enthalpy, velocity and pressure were set at 1×10^{-8} J, 1×10^{-8} m/s and 1×10^{-8} Pa, respectively, for each time step. In each case the simulations were run until a (quasi-)thermally-equilibrated state was reached, typically requiring up to approximately 30 seconds of simulation time. Thermal equilibration was judged by calculating the convective heat loss from the walls of the cavity interior at each time step. The normal temperature gradient at the walls was integrated over the cavity interior to determine the heat loss via the user generated OpenFOAM executable “wallHeatFluxRho” [6]. The single heat loss value presented here corresponds to a time-average from the (quasi-)steady state reached in each simulation.

Turbulence models, such as the commonly used $k-\epsilon$ closure scheme, were not used for two reasons. Firstly, there is a lack of experimental data to validate implementation of common closure schemes for buoyancy-driven flows. Secondly, there is evidence that such models would over predict the spreading rate of axisymmetric jets, such as the air curtain [13].

Meshing

The open source meshing software, Gmsh Version 2.6.2 [4], was used to generate all meshes. Hybrid meshes were used that consisted of unstructured tetrahedral elements in the external flow regions and structured hexahedral elements within the cavity. Hexahedral elements within the cavity were used to capture the thermal boundary layers at the hot cavity walls. The unstructured tetrahedral elements were suitable to represent the flows external to the cavity, and allowed the total number of elements in the domain to be maintained at a reasonable level. As shown in Figure 2, significant effort was made to ensure high resolution elements were present in all thermal boundary layers and regions expected to have a high velocity gradient. These high gradient regions are in the vicinity of the air curtain and inside the cavity, where the natural convective losses occur. The interface between structured

and unstructured elements is shown in Figure 3. It is worth noting that the heat loss and convective flow in the cavity interior was not influenced by a relatively coarse resolution of the heated exit plume remote from the cavity.

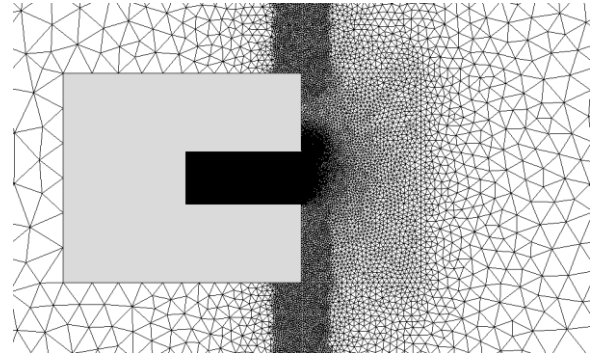


Figure 2. Meshing Approach – Overview

For these studies the mesh resolution was increased until changes in the convective heat loss were less than 1%. The mesh resolution required to achieve this was determined for the most unsteady case (a horizontal cavity; $\Theta = 0^\circ$), and that mesh applied to models with inclined cavity orientations. The structured meshing region within the cavity maintained an element aspect ratio of approximately 1 in all models. To achieve mesh invariance with the air curtain required 98,649 elements, with 0.47 mm square thermal boundary elements. Models without the air curtain required 22,272 elements, with 0.86 mm square, thermal boundary layer elements.

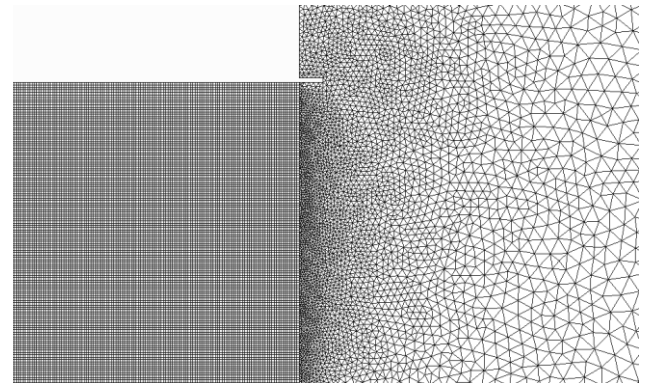


Figure 3. Structured and Unstructured Mesh Interface

Results and Discussion

Base Case Investigation

An initial set of simulations without an air curtain was completed to provide a baseline for the cavity thermal performance. These two-dimensional models were compared with Paitoonsurikarn’s numerical works [9,10] and Taumoefolau’s experimental work [11,12]. The comparison is only approximate in the sense that it assumes the current two-dimensional results are scalable by cavity surface area to the three-dimensional results. However, such an approach was found previously by Paitoonsurikarn et al. [10] to yield reasonable results.

As demonstrated in Figure 4, the current results align well with Paitoonsurikarn’s two-dimensional simulations. Importantly, cavity-area scaling of the current results yields acceptable agreement with both Paitoonsurikarn’s three-dimensional simulations and Taumoefolau’s experimental data, often lying within the confidence intervals of the latter.

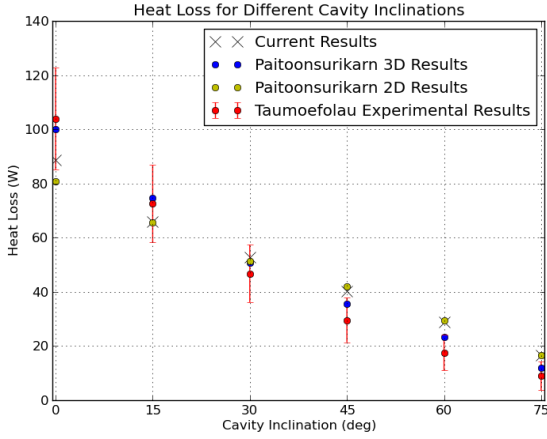


Figure 4. Comparison with Previous Studies

Effect of Cavity Inclination

The effectiveness of the air curtain can be defined [5] as

$$\epsilon = 1 - \frac{Q_{ACD}}{Q_0}, \quad (1)$$

where Q_{ACD} is the heat loss with the air curtain applied and Q_0 is the heat loss without. The baseline case results were used to give the Q_0 value for a given angle. The effectiveness as a function of air curtain velocity is shown for each cavity inclination in Figure 5. Note that the horizontal cavity had a maximum effectiveness of 54%, with an air curtain velocity of 1.4 m/s, as predicted by previous work [1, see discussion below].

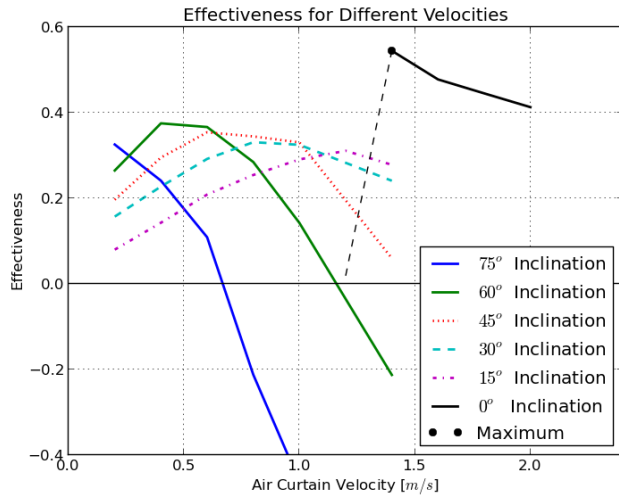


Figure 5. Effectiveness as a Function of Air Curtain Velocity

The air curtain effectiveness reaches a maximum in the range of 30% to 38% when the cavity is inclined between 15° and 75°, which is notably less than that for a horizontal cavity. Furthermore the effectiveness of the air curtain is demonstrated to become far more sensitive to air curtain velocity as cavity inclination increases.

Discussion

Previous work [1] has estimated the optimal air curtain velocity for a horizontal cavity using the concept of a “deflection modulus” D_m , a dimensionless number that measures the stability of the air curtain:

$$D_m = \frac{b_0 V^2 T_\infty T_w}{g H^2 T_0 (T_w - T_\infty)}, \quad (2)$$

where b_0 is the air curtain width, V is the air curtain velocity, T_∞ , T_w and T_0 is the ambient temperature, wall temperature and air

curtain temperature, respectively, g is the gravitational acceleration and H is the cavity height. The minimum deflection modulus $D_{m,min}$ corresponds to the air curtain velocity required to “seal” the cavity and prevent direct exchange of air from within the horizontal cavity. Importantly, the minimum air curtain velocity that can seal the cavity yields the greatest reduction in heat loss [1]. These optimal conditions are calculated using

$$D_{m,min} = \frac{-\sin \alpha_f - \sin \alpha_0 + 2 - 2\sqrt{(1 - \sin \alpha_f)(1 - \sin \alpha_0)}}{2(\sin \alpha_f - \sin \alpha_0)^2}, \quad (3)$$

$$\sin \alpha_f = 2.4 \sqrt{\frac{b_0}{H} \left(1 - 2.56 \frac{b_0}{H}\right)}, \quad (4)$$

where α_0 and α_f are the angles of the air curtain to the aperture plane at the top and bottom of the cavity, respectively. The predictions from Equations 2, 3 and 4 (with $\alpha_0 = 0^\circ$) yield an optimal air curtain velocity of 1.4 m/s, which was shown through these simulations to provide a maximum effectiveness of 54%, in excellent agreement with the current theory for air curtain devices.

The dependence in Figure 5 of air curtain effectiveness on inclination angle and air curtain velocity arises because of the interaction of the jet with the stratification in the cavity. In the absence of an air curtain, significant temperature stratification develops as a stagnant region trapped within the cavity receiver (Figure 6) for all angles of inclination slightly greater than 0°.

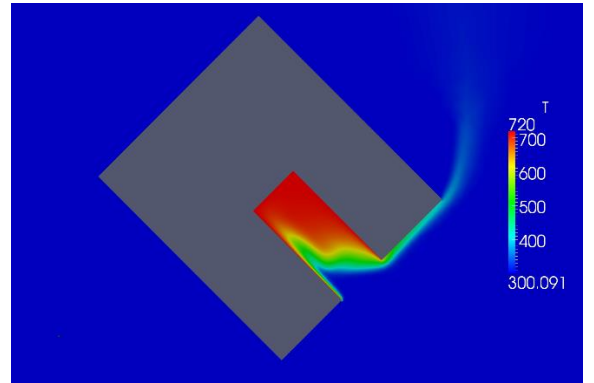


Figure 6. 45° Inclined Cavity without an Air Curtain

Optimal operation of an air curtain for horizontally connected volumes relies on a jet that is sufficiently strong to remain coherent across the cavity aperture, impacting against the far wall and thus acting to seal the cavity from the convective loss. However, this principle no longer provides the optimum operating condition for an inclined cavity. For the 45° cavity in Figure 5, the air curtain is most effective with a jet velocity of approximately 0.6 m/s (see Figure 7), rather than the 1.4 m/s predicted [1] when no account is taken of cavity inclination. Although increases in jet velocity beyond 0.6 m/s tend to seal the cavity in the traditional sense, this comes at the expense of disturbing the trapped stratification and increasing the convection losses.

The most effective air curtain strength at a given inclination angle results in a marginal increase in the stagnant region (Figure 7) and a reduction in the convective heat loss (by 35% for the 45° case). Figure 5 indicates that as cavity inclination is increased, the sealing effect comes at greater detriment to cavity performance and a greater reduction in air curtain velocity is appropriate.

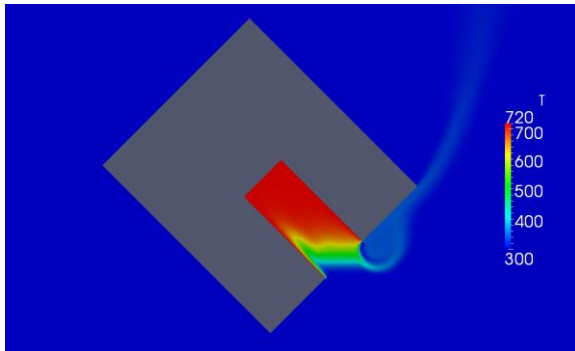


Figure 7. 45° Inclined Cavity with an Air Curtain ($V_0=0.6 \text{ m}\cdot\text{s}^{-1}$)

Comparison with experiments

Qualitative comparison of the two-dimensional convective flows presented here was possible using experimental data acquired by Tim Lindley [personal communication]. Lindley used variations in salinity and a nominally two-dimensional model cavity immersed in water to represent the interaction of receiver cavity convection with an air curtain across the aperture (Figure 8; the red-dyed fresh water is analogous to heated air). The Rayleigh number in the water experiment was designed to simulate a cavity heated to approximately 500°C. Despite differences in the physical system, a qualitative comparison of the convective flows in Figures 7 and Figure 8 highlights much in common.

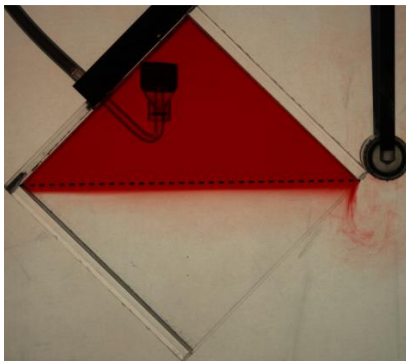


Figure 8. 45° Inclined model cavity immersed in water – optimal “air” curtain operation (courtesy of Tim Lindley)

The visualisation in Figure 8, shows that the optimised configuration at 45° does not completely seal the cavity. The visible convective flow escaping the cavity is consistent with the temperature field shown in Figure 7. The dotted line in Figure 8 indicates the extent of the stagnant region without an air curtain, and it is apparent that this region is marginally enlarged in both cases.

Conclusions

Two-dimensional CFD models indicate that an air curtain can be used to reduce convective heat loss in open-ended cavities. The air curtain is shown to be most effective for a horizontal cavity, with a reduction in heat loss of 54% – in agreement with previous work. For inclined cavities it was shown that the optimal reduction in heat loss remains relatively constant at between 30% and 38% over the range of inclination angles. As cavity inclination angle increases, optimal operation of the air curtain requires lower jet velocities that do not unduly disturb the temperature structure. Unlike a horizontal cavity, however, a sudden transition in heat loss reduction is not observed. These results are qualitatively

consistent with experimental observations but further work to develop a three-dimensional CFD model is required.

Acknowledgments

GH was supported by Australian Research Council Future Fellowship FT100100869. Numerical computations were conducted using the National Facility of the Australian National Computational Infrastructure.

References

- [1] Belleghem, M., Verhaeghe, G., T’Joel, C., Huisseune, H., De Jaeger, P., De Paepe, M., Heat Transfer Through Vertically Downward-Blowing Single-Jet Air Curtains for Cold Rooms, in *Heat Transfer Engineering*, 2012, 1196-1206.
- [2] Burgess, G., Lovegrove, K., Mackie, S., Zapata, J, Pye, J., *Direct Steam Generation using the SG4 500m 2 Paraboloidal Dish Concentrator*. <http://solar-thermal.anu.edu.au/files/2011/09/burgess-2011-dsg-sg4.pdf>, 2011.
- [3] Costa, J., Oliveira, L., Silva, M., Energy savings by aerodynamic sealing with a downward-blowing plane air curtain: A numerical approach, in *Energy and Buildings*, 2006, 1182-1193.
- [4] Geuzaine, C., Remacle, J., *Gmsh: a three-dimensional finite element mesh generator with built-in pre-and post-processing facilities*, 2009.
- [5] Goncalves, J., Costa, J., Figueiredo, A., Lopes, A., CFD modelling of aerodynamic sealing by vertical and horizontal air curtains, in *Energy and Buildings*, 2012, 153-160
- [6] Guilherme, S., *wallHeatFluxRho.C.*, <http://is.gd/XBdApy>, 2010, Revision Date: 5 December 2010, Accessed: October 2013
- [7] Holman, J., *Heat Transfer*, McGraw-Hill Inc., New York, tenth edn, 2010.
- [8] OpenFOAM Foundation, *OpenFOAM – User Guide*, Paris, France, May 2012.
- [9] Paitoonsurikarn, S., *Study of a Dissociation Reactor for an Ammonia-Based Solar Thermal System*, PhD. Thesis, The Australian National University, 2006.
- [10] Paitoonsurikarn, S., Lovegrove, K., Hughes, G. & Pye, J. 2011 Numerical investigation of natural convection loss from cavity receivers in solar dish applications, in *Journal of Solar Energy Engineering*, 2004, 133, doi: 10.1115/1.4003582.
- [11] Taumofolau, T., *Experimental Investigation of Convection Loss from a Model Solar Concentrator Cavity*, M.Phil. Thesis, The Australian National University, 2004.
- [12] Taumofolau, T., Paitoonsurikarn, S., Hughes, G. & Lovegrove, K. 2004 Experimental investigation of natural convection heat loss from a model solar concentrator cavity receiver, in *Journal of Solar Energy Engineering*. 126, 801–807.
- [13] Versteeg, H.K., Malalasekera, W., *An Introduction to Computational Fluid Dynamics – The Finite Volume Method*, Pearson Education Limited., Harlow, second edn, 200